Earth and Planetary Science Letters 429 (2015) 20–24

Contents lists available at ScienceDirect

Earth and Planetary Science Letters

www.elsevier.com/locate/epsl

Climate stability of habitable Earth-like planets

Kristen Menou [a,b,*]

[a] Centre for Planetary Sciences, Department of Physical & Environmental Sciences, University of Toronto at Scarborough, Toronto, Ontario M1C 1A4, Canada
[b] Department of Astronomy & Astrophysics, University of Toronto, Toronto, Ontario M5S 3H4, Canada

ARTICLE INFO

Article history:
Received 21 November 2014
Received in revised form 6 July 2015
Accepted 23 July 2015
Available online 10 August 2015
Editor: C. Sotin

Keywords:
climate

ABSTRACT

The carbon–silicate cycle regulates the atmospheric CO_2 content of terrestrial planets on geological timescales through a balance between the rates of CO_2 volcanic outgassing and planetary intake from rock weathering. It is thought to act as an efficient climatic thermostat on Earth and, by extension, on other habitable planets. If, however, the weathering rate increases with the atmospheric CO_2 content, as expected on planets lacking land vascular plants, the carbon–silicate cycle feedback can become severely limited. Here we show that Earth-like planets receiving less sunlight than current Earth may no longer possess a stable warm climate but instead repeatedly cycle between unstable glaciated and deglaciated climatic states. This has implications for the search for life on exoplanets in the habitable zone of nearby stars.

1. Introduction

It is generally thought that the carbon–silicate cycle acts as a stabilizing feedback and a powerful thermostat for the Earth climate, guaranteeing surface liquid water conditions. Above freezing temperatures, rock weathering occurs faster at higher temperatures, which reduces the CO_2 atmospheric partial pressure, pCO_2, and cools down the climate. Conversely, on a frozen planet that temporarily lacks weathering, atmospheric CO_2 builds up from continued volcanic outgassing, which warms up the climate until surface liquid water and weathering conditions are restored (Walker et al., 1981; Kasting et al., 1993; Kump et al., 2000). Such pCO_2 build up is in fact the leading scenario for the deglaciation of Earth following a snowball event (Kirschvink, 1981; Hoffman et al., 1998; Hoffman and Schragg, 2002). Generalizations of these concepts to Earth-like planets around other stars are central to the definition of their liquid water habitable zone (Kasting et al., 1993; Forget and Pierrehumbert, 1997; Kopparapu et al., 2013). In particular, planets subject to modest levels of insolation are expected to achieve temperate conditions with liquid water at the surface by building up massive enough CO_2 atmospheres (Kasting et al., 1993; Williams and Kasting, 1997; Selsis et al., 2007).

Experimental data, theoretical arguments and paleoclimate modeling suggest that the rate of CO_2 intake via rock weathering by a planet lacking land vascular plants increases with the atmospheric CO_2 content, pCO_2 (Walker et al., 1981; Kump et al., 2000; Schwartzman and Volk, 1989; Berner, 1992, 1994; Berner and Kothavala, 2001). This feature of lifeless planets or planets with only primitive forms of life is important because it will limit the buildup of CO_2 at high values. As a result, the climate thermostat due to the carbon–silicate cycle should become less efficient on weakly-insolated Earth-like planets located in the outer regions of the habitable zone.

2. Climate-weathering models

To address this issue quantitatively, we model Earth-like climates on planets around Sun-like stars with a zero-dimensional, energy balance model that equates the net insolation and thermal radiation fluxes,

$$\frac{S}{4}\left[1-\alpha(T_{\rm surf}, p{\rm CO}_2)\right] = OLR(T_{\rm surf}, p{\rm CO}_2), \quad (1)$$

where S is the insolation flux, α is the planetary Bond albedo and OLR is the outgoing longwave radiation flux emitted by the planet. OLR and α are functions of the surface temperature, $T_{\rm surf}$, and pCO_2, derived from radiative–convective climate models (Williams and Kasting, 1997) (see Appendix A for details).

While we assume that the climate reaches thermal equilibrium rapidly, by virtue of Equation (1), the slower CO_2 compositional equilibrium is not imposed a priori in our models. Rather, pCO_2 is evolved on the relevant geological timescales according to

$$\frac{d}{dt}p{\rm CO}_2 = V - W(T_{\rm surf}, p{\rm CO}_2), \quad (2)$$

* Corresponding author at: Centre for Planetary Sciences, Department of Physical & Environmental Sciences, University of Toronto at Scarborough, Toronto, Ontario M1C 1A4, Canada.
E-mail address: kristen.menou@utoronto.ca.

http://dx.doi.org/10.1016/j.epsl.2015.07.046
0012-821X/

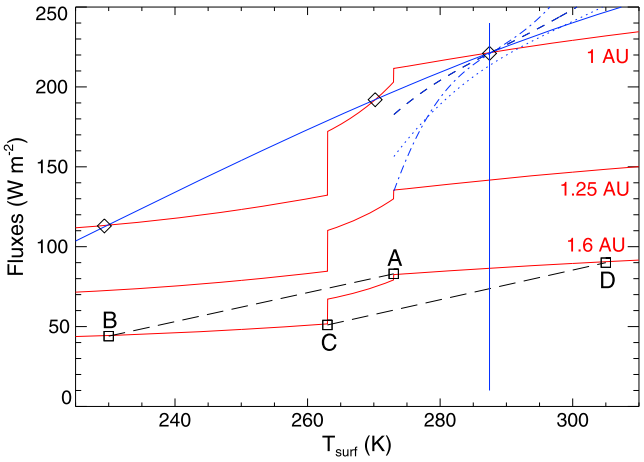

Fig. 1. Climate at global radiative equilibrium for an Earth-like planet. Red lines show the albedo-corrected insolation (heating) flux as a function of surface temperature, $T_{\rm surf}$, at 1 AU (top), 1.25 AU (middle) and 1.6 AU (bottom) from a Sun-like star. Blue lines show the infrared cooling flux (*OLR*) according to various scenarios for the atmospheric CO_2 content (slanted solid line: fixed pCO_2 model; dashed: $\beta = 0.5$ weathering model; dotted: $\beta = 0.5$ weathering model with 3 times larger CO_2 outgassing rate; dash-dotted: $\beta = 0.25$ weathering model; vertical solid: $\beta = 0$ weathering model). When no stable climate exists at large orbital distances (absent blue–red intersections), the climate must repeatedly cycle through points A–B–C–D shown in the 1.6 AU case, with a slow pCO_2 build-up (B–C), a transition to a hot climate (C–D), a weathering period with decreasing pCO_2 (D–A) and a transition to global glaciation (A–B). (For interpretation of the references to color in this figure legend, the reader is referred to the web version of this article.)

where V is the global CO_2 volcanic outgassing rate (estimated as $V_\oplus = 7$ bars/Gyr for Earth, Abe et al., 2011) and W is the rate of CO_2 intake by the solid planet via rock weathering. The functional form of W is adapted from Earth studies for pre-vascular plant conditions (Berner and Kothavala, 2001):

$$\frac{W}{W_\oplus} = \left(\frac{p{\rm CO}_2}{p_\oplus}\right)^\beta e^{[k_{\rm act}(T_{\rm surf}-288)]} \times \left[1 + k_{\rm run}(T_{\rm surf} - 288)\right]^{0.65}, \quad (3)$$

where $p_\oplus = 330$ μbar is the pre-industrial pCO_2 level, $W = W_\oplus \equiv V_\oplus$ for $T_{\rm surf} = 288$ K, $k_{\rm act} = 0.09$ is related to an activation energy and $k_{\rm run} = 0.045$ is a runoff efficiency factor. Varying Berner and Kothavala (2001) $k_{\rm act}$ in the 0.06–0.135 range and $k_{\rm run}$ in the 0.025–0.045 range has only a minor quantitative impact on our results. Values of $\beta = 0.25$–1 have been considered in the literature (Kump et al., 2000; Berner, 1992; Abbot et al., 2012; Pierrehumbert, 2010) for the dependence of weathering on pCO_2 in the absence of land vascular plants. We use $\beta = 0.5$ (default) and 0.25 in this work. Note that equations (1) and (2) are coupled through pCO_2 and $T_{\rm surf}$.

3. Climate solutions

3.1. Steady–state solutions

Steady–state climate solutions, satisfying both radiative (Equation (1)) and weathering equilibrium ($d/dt \equiv 0$ in Equation (2)) are represented in Fig. 1 by intersecting cooling and heating curves. Solid red lines in Fig. 1 show the albedo-corrected insolation flux (LHS of Equation (1)) received by a planet located at 1, 1.25 and 1.6 AU from a Sun-like star as a function of surface temperature.[1] Net insolation drops precipitously from 273 K to 263 K as the planetary surface freezes and the albedo reaches ∼0.65. The various blue lines in Fig. 1 represent the *OLR* cooling flux (RHS of Equation (1)) according to various scenarios for the atmospheric CO_2 content.

A standard model with pCO_2 arbitrarily fixed at $p_\oplus = 330$ μbar (i.e. not constrained by Equation (2)) is represented by the slanted solid blue line. As is well known (Budyko, 1969; Sellers, 1969; North et al., 1981), three steady–state climate solutions exist in such a model for an Earth-like planet at 1 AU, as indicated by diamonds where the red and blue curves intersect. Earth's current climate ($T_{\rm surf} \simeq 288$ K) and a globally-frozen state ($T_{\rm surf} \simeq 229$ K) are both stable, while the intermediate state ($T_{\rm surf} \simeq 270$ K) is thermally unstable.

However, when pCO_2 is also required to satisfy weathering equilibrium (Equation (2)), steady–state climate + weathering solutions only exist above freezing temperatures since weathering stops operating on a frozen planet. A model including weathering without any pCO_2 dependence (Williams and Kasting, 1997) ($\beta = 0$ in Equation (3)) is represented by the vertical solid blue line in Fig. 1. In such a model, weathering equilibrium enforces a unique surface temperature, set by requiring that weathering balances volcanic outgassing in Equation (2), and pCO_2 is only indirectly constrained by the constant $T_{\rm surf}$ requirement.

On the other hand, when the weathering rate depends on both pCO_2 and $T_{\rm surf}$, noticeable bends appear in the blue cooling curves shown in Fig. 1. Indeed, in this class of models, the reduced efficiency of weathering at low temperatures must be balanced by large pCO_2 values to match the volcanic outgassing rate V. The weaker the weathering pCO_2 dependence, the stronger is the pCO_2 build-up at low surface temperatures (compare $\beta = 0.5$ and 0.25 models represented by the dashed and dash-dotted lines in Fig. 1, respectively). A planet with a larger volcanic CO_2 outgassing rate (Kite et al., 2009) achieves a warmer stable climate ($T_{\rm surf} \simeq 292$ K for $V = 3V_\oplus$ and adopting our default weathering parameters, which is the case shown as a dotted line in Fig. 1).

Interestingly, stable climate + weathering solutions can cease to exist at low insolation levels, such as the 1.25 and 1.6 AU cases shown in Fig. 1, for a strong enough dependence of the weathering rate on pCO_2. For example, we find that blue curves no longer intersect with heating (insolation) lines beyond 1.077 AU if $\beta = 0.5$ and beyond 1.25 AU if $\beta = 0.25$. Conversely, a very weak weathering dependence on pCO_2 ($\beta < 0.1$), including the singular case $\beta = 0$ (vertical solid blue line in Fig. 1), do permit stable climate + weathering solutions at almost arbitrarily low insolation levels (Williams and Kasting, 1997). Low β values may be the relevant limit for planets where land vascular plants are widespread (Kump et al., 2000; Schwartzman and Volk, 1989; Berner, 1992, 1994; Berner and Kothavala, 2001; Pierrehumbert, 2010). On the other hand, for values of $\beta \sim 0.25$–0.5 appropriate for planets lacking land vascular plants (Kump et al., 2000; Schwartzman and Volk, 1989; Berner, 1992, 1994; Berner and Kothavala, 2001; Pierrehumbert, 2010), the bending of cooling curves seen in Fig. 1 also implies that at fixed volcanism rate, V, less insolated planets achieve climate + weathering equilibrium at gradually lower $T_{\rm surf}$ values. For example, in the case $\beta = 0.25$, equilibrium is only marginally achieved above freezing temperatures at 1.25 AU, as shown in Fig. 1. At low enough insolation levels (far enough away from the star), climate + weathering equilibrium is no longer possible above freezing temperatures, which implies that weathering equilibrium is unattainable.

[1] Even though the planetary albedo α in Equation (1) depends on pCO_2, we find that this dependence is quantitatively negligible for $pCO_2 \ll 0.2$ bar. For simplicity, we plot heating (red) curves in this low pCO_2 limit in Fig. 1, which is indeed satisfied by all the cooling (blue) curves shown. All our other results fully account for the α–pCO_2 dependence.

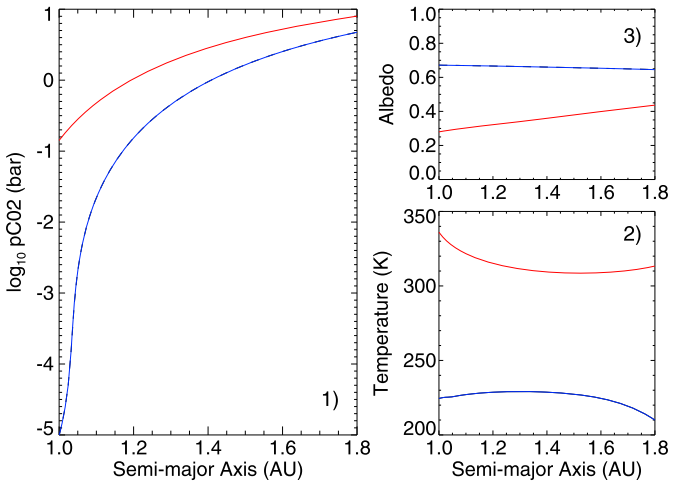

Fig. 2. Values of atmospheric partial CO_2 pressure (1), surface temperature (2) and planetary albedo (3) at extremes of the climate cycle illustrated in Fig. 1, as a function of orbital distance from a Sun-like star. Blue curves correspond to point B (cold, high albedo, low pCO_2) and red curves to point D (hot, low albedo, high pCO_2) of the cycle shown in Fig. 1. (For interpretation of the references to color in this figure, the reader is referred to the web version of this article.)

On planets lacking weathering equilibrium, the climate must repeatedly cycle through a succession of radiative equilibria as illustrated in Fig. 1: rapid transition from marginal to full glaciation (A → B, at fixed pCO_2), slow build-up of pCO_2 caused by volcanic outgassing in the absence of weathering (B → C), rapid transition to a deglaciated state (C → D, at fixed pCO_2) and gradual pCO_2 decay under the action of weathering (D → A), until the cycle repeats again with full glaciation. The general properties of the four critical points A–B–C–D of this climate cycle, which are independent of details of the weathering model, are quantified in Fig. 2 as a function of orbital distance from a Sun-like star. Blue curves correspond to the coldest cycle point with the lowest pCO_2 value, B, while the red curves correspond to the hottest point with the highest pCO_2 value, D.

Fig. 2 shows that Earth-like planets at larger orbital distances glaciate and deglaciate at larger pCO_2 values. A deglaciation with $pCO_2 \simeq 0.14$ bar at 1 AU is consistent with values reported for snowball Earth deglaciation (Hoffman and Schragg, 2002). Planets beyond 1.3 AU support massive (>0.3 bar) CO_2 atmospheres throughout their climate cycle. Planets in the frozen state have albedos ≃0.65, while the albedo of unfrozen planets rises from ≃0.3 to 0.45 in the 1–1.8 AU range, from an increasing atmospheric scattering contribution. The extremes of surface temperature along the cycle vary modestly with insolation level, with $T_{surf} \simeq 210$–225 K at the coldest point and 310–330 K at the hottest point.

3.2. Climate cycles

Explicit time-dependent integrations of the system of Equations (1)–(3) reveal details of the climate cycle illustrated in Fig. 1. We initiated these integrations at the hot, high pCO_2 (weathering-independent) point D and confirmed that Earth-like planets receiving sufficiently large insolation fluxes settle to a steady–state warm climate solution after relaxation to weathering equilibrium. By contrast, planets at large enough orbital distances (low enough insolation levels) experience large amplitude climate cycles, as anticipated from our discussion of equilibrium solutions in relation to Fig. 1.

Fig. 3 shows six illustrative examples (A–F) of such climate cycles, shown in terms of variable T_{surf} and pCO_2 curves. Most of the cycle time is spent in the frozen state, during which pCO_2 build-up

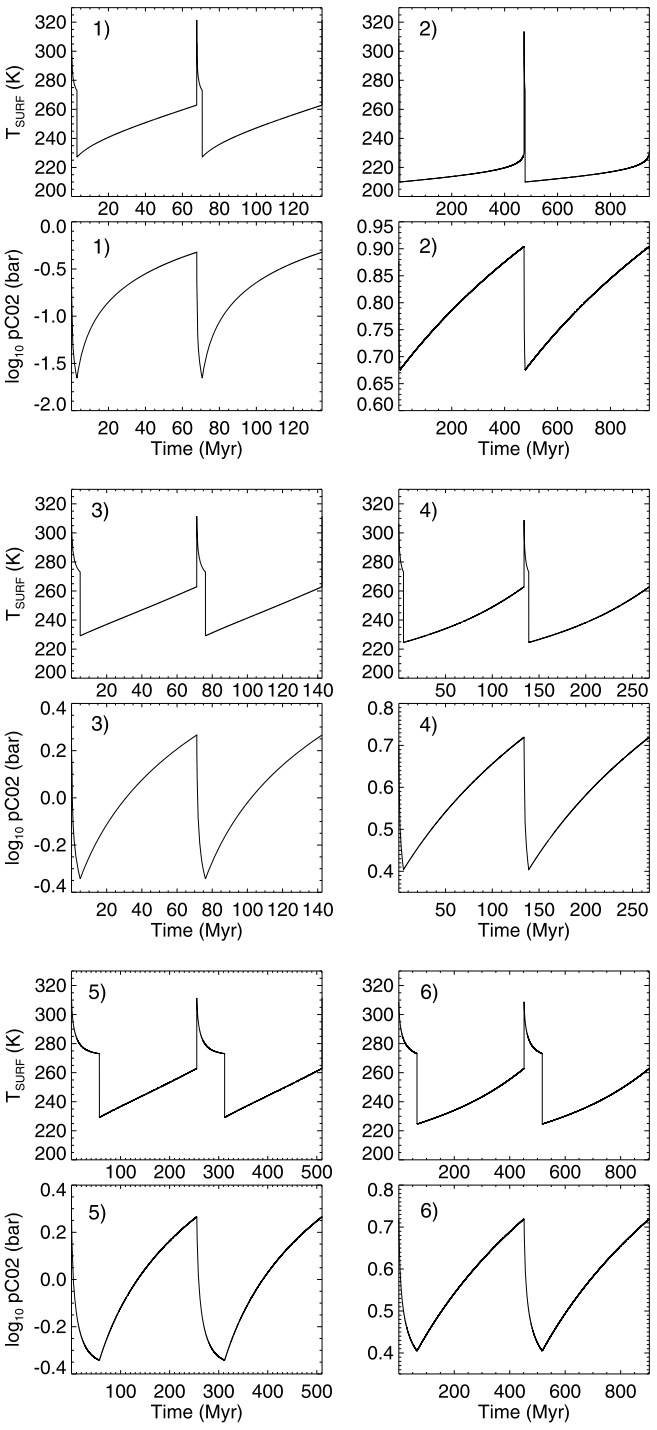

Fig. 3. Six examples of time-evolved climate cycles, with two full cycles shown in each case. For each model (1–6), the evolution of atmospheric partial CO_2 pressure (lower panel) and surface temperature (upper panel) are shown. Model 1: Default weathering model at 1.1 AU ($\beta = 0.5$ in Equation (3)). Model 2: Default weathering model at 1.8 AU. Model 3: 3 times larger CO_2 outgassing rate at 1.3 AU. Model 4: 3 times larger CO_2 outgassing rate at 1.6 AU. Model 5: Weaker pCO_2 weathering dependence ($\beta = 0.25$) at 1.3 AU. Model 6: Weaker pCO_2 weathering dependence ($\beta = 0.25$) at 1.6 AU. Increasing the CO_2 outgassing rate shortens the duration of the cold, CO_2 build-up phase. Weakening the weathering pCO_2 dependence ($\beta = 0.25$ rather than 0.5) lengthens the duration of the hot weathering phase, resulting in a much larger fraction of time spent with surface liquid water.

is slow compared to the fast weathering that occurs at above-freezing temperatures. In model 1, 4.6% of the 70 Myr cycle is spent in a warm state with surface liquid water. The corresponding numbers are 0.8% of 477 Myr in model 2, 7.5% of 76 Myr in model

3, 3.9% of 139 Myr in model 4, 28% of 312 Myr in model 5 and 17% of 517 Myr in model 6. Faster weathering at higher T_{surf} also implies that most of the time in the unfrozen state is spent just above freezing temperatures, near the lowest pCO_2 levels covered during the cycle. For a fixed volcanic outgassing rate, V, the climate cycle duration increases with decreasing insolation because larger absolute pCO_2 values must be reached for climate transitions to occur (Fig. 2). Decreasing insolation also reduces the fraction of cycle time spent with surface liquid water by the planet, although this can be compensated for by stronger volcanic outgassing. A weaker pCO_2 weathering dependence (lower β) lengthens the duration of the unfrozen state since the decline in pCO_2 with time has less of an effect on the weathering rate.

To summarize, a temperature-only dependence of the weathering rate ($\beta = 0$) uniquely ties the surface temperature to the volcanic outgassing rate V via Equation (2). A more general dependence on pCO_2 ($\beta > 0$) leads to a richer set of climate solutions, including unstable climate cycles at low enough insolation levels, when weathering equilibrium ceases to exist. These results are not specific to the weathering functional form adopted in Equation (3), in the sense that other weathering laws with a positive dependence on pCO_2 and T_{surf} would lead to qualitatively similar climate behaviors.

4. Conclusions

The key new feature of our analysis is the lack of stable climates on Earth-like planets lacking land vascular plants, at low enough insolation levels (see also Kadoya and Tajika, 2014). This suggests that a subset of Earth-like planets located in the outer regions of habitable zones may be preferentially found in a frozen, rather than deglaciated, state.[2] A globally frozen state might be observationally inferred from the very high albedo and the correspondingly low water content of the planet's atmosphere. According to these results, some Earth-like planets in the outer habitable zone would also be caught in a transiently warm state with surface liquid water present only infrequently.

The link between unstable climate cycles and the emergence and evolution of life on weakly-insolated Earth-like planets is unclear but possibly important. A reduced amount of time with surface liquid water on planets experiencing climate cycles could in principle slow down the emergence and/or evolution of life (see however Planavsky et al., 2010). On the other hand, life itself could strongly impact the weathering process on weakly-insolated Earth-like planets, as it seems to have done on early Earth (Kump et al., 2000; Schwartzman and Volk, 1989; Berner, 1992, 1994; Berner and Kothavala, 2001; Pierrehumbert, 2010). Although considerable uncertainty remains, the ability of land vascular plants to regulate the soil pCO_2 level that is relevant to the weathering process, well above atmospheric pCO_2 levels, is consistent with these plants effectively decoupling the weathering rate from the atmospheric pCO_2 level (Kump et al., 2000; Schwartzman and Volk, 1989; Berner, 1992, 1994; Berner and Kothavala, 2001; Pierrehumbert, 2010), leading to $\beta \to 0$ in Equation (3). As a result (Fig. 1, vertical line), the climate of weakly-insolated Earth-like planets could be stabilized against transient cycles once the presence of land vascular plants becomes widespread. This would constitute a strong example of life exerting a feedback on its environment.

Based on these results, one can envision a typical evolutionary path for a habitable planet in orbit around a star that is gradually brightening over time. Repeated snowball events should occur at earlier times, when insolation is weak and land vascular plants are absent. They should disappear at later times once insolation is strong enough and/or land vascular plants become widespread. In the case of Earth, the Paleoproterozoic and Neoproterozoic snowball events have been interpreted as being caused by an increase in atmospheric O_2 levels and a corresponding decrease in CH_4 levels (Kasting, 2005; Pavlov et al., 2003), rather than the climate cycles highlighted in this work.

[2] It is unclear whether such glaciated states would correspond to hard snowballs or milder versions (McKay, 2000; Pollard et al., 2005; Abbot et al., 2011).

Acknowledgements

This work was supported by the Natural Sciences and Engineering Research Council of Canada. The author is grateful to J. Leconte and D. Valencia for comments on the manuscript.

Appendix A. Energy balance climate model

We model the climate of Earth-like planets with a zero-dimensional reduction of a one-dimensional energy balance model (Williams and Kasting, 1997). The model assumes Earth parameters unless otherwise specified (e.g., surface gravity, land/ocean fraction and nitrogen contribution to the total atmospheric mass). Greenhouse effect from atmospheric H_2O and CO_2 are included, with an atmospheric vapor pressure set by surface evaporation (temperature).

The top-of-atmosphere albedo and the outgoing longwave radiation flux are modeled as polynomial fits to a large number of radiative–convective models (Williams and Kasting, 1997). The polynomial fits are functions of surface temperature, partial CO_2 pressure, solar zenith angle and surface albedo. Simple prescriptions for snow/ice coverage, surface albedo and water cloud coverage are adapted from Williams and Kasting (1997). For simplicity, we fix the cosine of the zenith angle to $\mu = 0.4$ and the albedo of ice-free oceans to 0.07 in all the models presented here. We also smooth out the top-of-atmosphere albedo polynomials near the 280 K transition to improve the continuity of the albedo function with temperature.

Based on published results (Kasting et al., 1993), we expect that our results would be quantitatively different, but remain qualitatively valid, for planets that differ modestly from Earth in terms of their surface gravity, land/ocean fraction and/or nitrogen atmospheric content. Note that it has been suggested that weathering does not strongly depend on land/ocean fraction on an Earth-like planet (Abbot et al., 2012). Given the prescriptions adopted, our models are specialized to planets orbiting Sun-like stars. Planets orbiting low-mass M-dwarf stars would experience reduced ice-albedo feedback because of the more reddish nature of the stellar light (Joshi and Haberle, 2012). Preliminary tests indicate that a reduced ice albedo leads to comparatively shorter and lower amplitude climate cycles on such planets.

The energy balance model employed here may not be fully reliable beyond 1.3–1.4 AU, where CO_2 clouds are expected to form and influence the climate (Williams and Kasting, 1997; Selsis et al., 2007). Although the most massive CO_2 atmospheres found in our models only marginally approach hard limits on CO_2 condensation (von Paris et al., 2013), it is also expected that the ice albedo feedback ceases to operate on planets with very massive CO_2 atmospheres ($pCO_2 > 10$ bars; Wordsworth et al., 2011).

Appendix B. Model simplifications and limitations

Our models are idealized in a number of important ways. In addition to the simplified, zero-dimensional treatment of climate described above, which suggests the possibility of richer behaviors in higher complexity, three-dimensional climate models, our treatment of weathering processes is intentionally simple, in order to

isolate they key factors that determine climate stability. We ignore seafloor weathering (Abbot et al., 2012) and the mantle CO_2 cycle (Sleep and Zahnle, 2001).

The absolute calibration of weathering rates in the absence of land vascular plants is unknown, but it is thought to be less than in their presence (Schwartzman and Volk, 1989). For concreteness, we have chosen to calibrate weathering fluxes in our models using current Earth (Berner, 1994; Berner and Kothavala, 2001) (Equation (3)). We note that in a model admitting steady–state solutions, a factor three decrease in the weathering rate is equivalent to a factor three increase in the volcanic outgassing rate (see Equation (2)), which is one of the cases shown in Fig. 1 (dotted blue line). Such a model retains the main qualitative feature highlighted in this work, which is the disappearance of stable climates solutions at low enough insolation levels (beyond 1.2 AU for the dotted blue line shown in Fig. 1). Different calibrations in weathering rates and/or volcanic outgassing rates will thus affect our results quantitatively, but our main conclusions should remain valid.

More generally, a planet is likely to change its weathering regime gradually over time, as different forms of life emerge and spread over its surface (Kump et al., 2000; Berner, 1992). Our models have intentionally focused on the distinction between the absence and presence of land vascular planets, which exemplifies the interplay between life, weathering processes and climate stability.

References

Abbot, D.S., Cowan, N.B., Ciesla, F.J., 2012. Indication of insensitivity of planetary weathering behavior and habitable zone to surface land fraction. Astrophys. J. 756, 178–191.

Abbot, D.S., Voigt, A., Koll, D., 2011. The Jormungand global climate state and implications for Neoproterozoic glaciations. J. Geophys. Res. D 116, D18103, 14 pp.

Abe, Y., Abe-Ouchi, A., Sleep, N.H., Zahnle, K.J., 2011. Habitable zone limits for dry planets. Astrobiology 11, 443–460.

Berner, R.A., 1992. Geochim. Cosmochim. Acta 56, 3225–3231.

Berner, R.A., 1994. Geocarb II: a revised model of atmospheric CO_2 over Phanerozoic time. Am. J. Sci. 294, 56–91.

Berner, R.A., Kothavala, Z., 2001. Geocarb III: a revised model of atmospheric CO_2 over Phanerozoic time. Am. J. Sci. 301, 182–204.

Budyko, M.I., 1969. The effect of solar radiation variations on the climate of the Earth. Tellus 21, 611–619.

Forget, F., Pierrehumbert, R.T., 1997. Warming Early Mars with carbon dioxide clouds that scatter infrared radiation. Science 278, 1273–1276.

Hoffman, P.F., Kauffman, A.J., Halverson, G.P., Schragg, D.P., 1998. A Neoproterozoic snowball earth. Science 281, 1342–1346.

Hoffman, P.F., Schragg, D.P., 2002. The snowball Earth hypothesis. Terra Nova 14, 129–155.

Joshi, M.M., Haberle, R.M., 2012. Suppression of the water ice and snow albedo feedback on planets orbiting red dwarf stars and the subsequent widening of the habitable zone. Astrobiology 12, 3–8.

Kadoya, S., Tajika, E., 2014. Conditions for oceans on Earth-like planets orbiting within the habitable zone: importance of volcanic CO_2 degassing. Astrophys. J. 790, 107–114.

Kasting, J.F., 2005. Methane and climate during the Precambrian era. Precambrian Res. 137, 119–129.

Kasting, J.F., Whitmire, D.P., Reynolds, R.T., 1993. Habitable zones around main sequence stars. Icarus 101, 108–128.

Kirschvink, J.L., 1981. In: Schopf, J.W., Klein, C. (Eds.), The Proterozoic Biosphere: A Multidisciplinary Study. Cambridge University Press, Cambridge, UK, pp. 51–52.

Kite, E.S., Manga, M., Gaidos, E., 2009. Geodynamics and rate of volcanism on massive Earth-like planets. Astrophys. J. 700, 1732–1749.

Kopparapu, R.K., et al., 2013. Habitable zones around main-sequence stars: new estimates. Astrophys. J. 765, 131–147.

Kump, L.R., Brantley, S.L., Arthur, M.A., 2000. Chemical weathering, atmospheric CO_2 and climate. Annu. Rev. Earth Planet. Sci. 28, 611–667.

McKay, C., 2000. Thickness of tropical ice and photosynthesis on a snowball earth. Geophys. Res. Lett. 27, 2153–2156.

North, G.R., Cahalan, R.F., Coakley Jr., J.A., 1981. Energy balance climate models. Rev. Geophys. Space Phys. 19, 91–121.

Pavlov, A.A., Hurtgen, M.T., Kasting, J.F., Arthur, M.A., 2003. Methane-rich Proterozoic atmosphere? Geology 31, 87–90.

Pierrehumbert, R.T., 2010. Principles of Planetary Climate. Cambridge Univ. Press, Cambridge.

Planavsky, N.J., Rouxel, O.J., Bekker, A., Lalonde, S.V., Konhauser, K.O., Reinhard, C.T., Lyons, T.W., 2010. The evolution of the marine phosphate reservoir. Nature 467, 1088–1090.

Pollard, D., Kasting, J.F., 2005. Snowball Earth: a thin-ice solution with flowing sea glaciers. J. Geophys. Res. C 110, C07010, 16 pp.

Schwartzman, D.W., Volk, T., 1989. Biotic enhancement of weathering and the habitability of Earth. Nature 340, 457–460.

Sellers, W.D., 1969. A global climatic model based on the energy balance of the Earth-atmosphere system. J. Appl. Meteorol. 8, 392–400.

Selsis, F., Kasting, J.F., Levrard, B., Paillet, J., Ribas, I., Delfosse, X., 2007. Habitable planets around the star Gliese 581? Astron. Astrophys. 476, 1373–1387.

Sleep, N.H., Zahnle, K., 2001. Carbon dioxide cycling and implications for climate on ancient Earth. J. Geophys. Res. 106, 1373–1400.

von Paris, P., Grenfell, J.L., Hedelt, P., Rauer, H., Selsis, F., Stracke, B., 2013. Atmospheric constraints for the CO_2 partial pressure on terrestrial planets near the outer edge of the habitable zone. Astron. Astrophys. 549, 94–102.

Walker, J.C.G., Hays, P.B., Kasting, J.F., 1981. A negative feedback mechanism for the long-term stabilization of Earth's surface temperature. J. Geophys. Res. 86, 9776–9782.

Williams, D.M., Kasting, J.F., 1997. Habitable planets with high obliquities. Icarus 129, 254–267.

Wordsworth, R.D., Forget, F., Selsis, F., Millour, E., Charnay, B., Madeleine, J.-B., 2011. Gliese 581d is the first discovered terrestrial-mass exoplanet in the habitable zone. Astrophys. J. 733, L48–L52.